Bacterial Characterization by Flow Cytometry

Abstract. *Bacteria were analyzed in a dual-beam flow cytometer after double staining with the fluorescent dyes chromomycin A3 and Hoechst 33258, which bind preferentially to DNA that is rich in guanine-cytosine and adenine-thymine, respectively. The measurements were indicative of the cellular DNA content and base composition, cell concentration, and proliferative state of the population. The ratio of the chromomycin A3 signal to the Hoechst 33258 signal increased with the guanine-cytosine content of the cellular DNA for the six cultured species measured, following expectation. Bacteria in urine from patients with urinary tract infections were characterized without interference from host cell DNA, debris, or other particulates.*

Flow cytometry, which has been applied extensively to mammalian cells and chromosomes (*1*), offers many possibilities for microbial measurement. The techniques of quantitative fluorescence cytochemistry make it possible to determine important structural and functional properties of individual cells with high precision at rates of 10^3 cells per second. More than one cellular property can be measured simultaneously. The objectives of the limited number of microbiological applications of flow cytometry have included the determination of ploidy levels, state of proliferation, state of protozoan infection, or glycoprotein cell wall composition in the case of yeast cells (*2*, *3*). Fluorescent stains for the cellular content of DNA, total nucleic acid, or protein were used, sometimes in combination; fluorescein-coupled lectins were used in the yeast cell wall studies (*3*).

We report here the application of a double fluorescent DNA staining method to bacteria. Originally developed for use with mammalian chromosomes (*4*), the technique uses chromomycin A3, having guanine-cytosine (GC) binding preference, and Hoechst 33258, having adenine-thymine (AT) binding preference. This stain combination provides information on the DNA base composition (that is, the proportion of GC and AT base pairs) as well as the DNA content. Bacterial species vary widely in base composition; GC values range between 25 and 70 percent of the total number of base pairs present in the DNA. We have analyzed six cultured bacterial species of clinical importance that differ in base composition and show that they can be distinguished on this basis. The flow cytometric ranking of the GC percentage strongly correlates with the biochemically determined GC percentages reported in the literature. We also show that bacteria in infected human urine can be measured in the same way without interference by host cellular and particulate material.

Cultured bacteria were collected by centrifugation and resuspended in 70 percent ethanol at concentrations of the order of 10^8 organisms per milliliter. Urine from patients with urinary tract infections was centrifuged and the bacterial pellet was resuspended in an equal volume of 70 percent ethanol. Fixed suspensions can be stored at 4°C for several months with no apparent degradation. For flow analysis, small portions of fixed bacterial suspension were added to a staining solution containing 3 μM Hoechst 33258, 10 μM chromomycin A3, 10 mM tris (pH 7.2), 150 mM NaCl, and 1.5 mM $MgCl_2$. Bacterial concentrations were typically 2×10^7 cells per milliliter in the final stained suspension, but variations in concentration from 10^7 to 10^8 cells per milliliter had no effect on the observed staining intensities.

Fluorescence from the doubly stained bacteria was measured with a dual-beam flow cytometer (*5*). The bacteria suspended in staining solution flow single file through a flow chamber and sequentially intersect a pair of laser beams, focused to elliptical spots of dimensions 150 by 20 μm spaced ~ 200 μm apart. The Hoechst 33258 was excited with 500 mW of the 337- to 356-nm lines from a Spectra-Physics 171-01 krypton ion laser, and the chromomycin A3 was excited with 500 mW of the 458-nm line of a Spectra-Physics 171-18 argon laser. The two fluorescence flashes emitted as a cell passes through the beams were collected with an *f*/1.0 lens and imaged through a Corning 3-71 filter (transmits above 480 nm) onto separate photomultipliers (EMI 9798 B). The resultant electrical pulses were amplified, processed, digitized, and stored in the memory of a two-parameter multichannel analyzer. Since the flow velocity is the same for all cells, the two signals from each cell are associated by their time separation. The 3-71 filter transmits almost all the chromomycin A3 fluorescence and about half the Hoechst 33258 fluorescence. Thus the photomultiplier focused on the 458-nm beam yields a signal (C) proportional to the

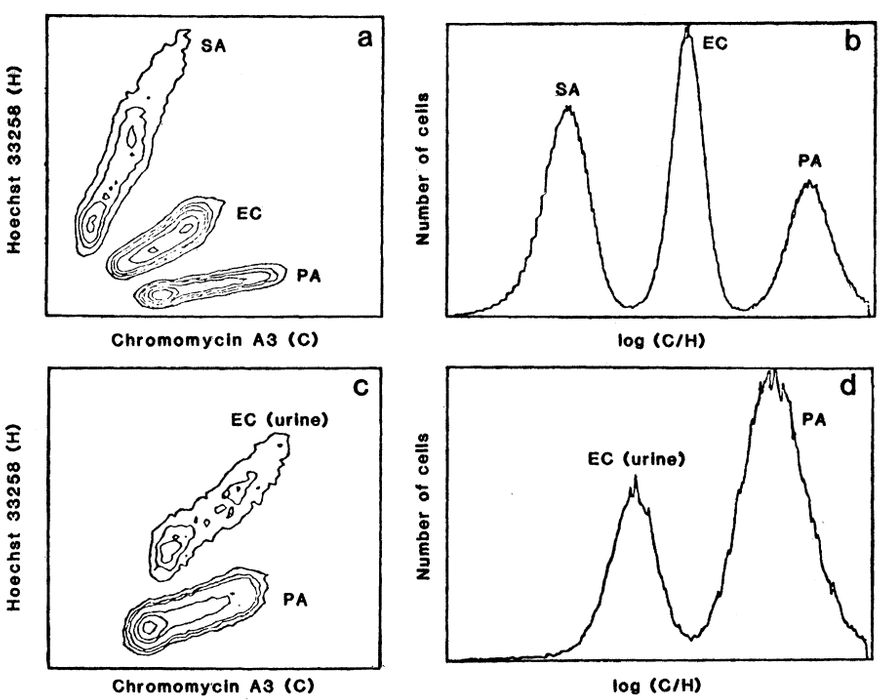

Fig. 1. (a) Bivariate contour plot of the fluorescence signals from a mixture of cultured *Staphylococcus aureus* (*SA*), *Escherichia coli* (*EC*), and *Pseudomonas aeruginosa* (*PA*) after double DNA staining with Hoechst 33258 (H) and chromomycin A3 (C). The peak height (number of cells) is indicated by the contours. (b) Distribution of the ratio of the two fluorescent signals, C/H, over the cell population of (a). (c) Bivariate contour plot of the fluorescence signals from *E. coli* from an infected urine sample after double DNA staining with Hoechst 33258 and chromomycin A3. Cultured *P. aeruginosa* was added as an internal standard. (d) Distribution of C/H over the cell population of (c).

chromomycin A3 content. The other photomultiplier, focused on the ultraviolet beam, measures about half the Hoechst 33258 fluorescence light that is collected plus the chromomycin A3 fluorescence stimulated by energy transfer from excited Hoechst 33258 molecules; this signal (H) is approximately proportional to the Hoechst 33258 content. Data were recorded at $\sim 10^3$ cells per second with a Nuclear Data model 6600 computer, which also generated both a real-time isometric display of the number of particles versus the two fluorescence signals and a display of the number of cells as a function of the ratio of the two fluorescence signals.

For quantitative measurements, standard aliquots of a reference suspension (*Escherichia coli* or *Pseudomonas aeruginosa*) were added to the stained sample so that fluorescence ratios could be determined relative to the reference strain independent of instrumental gain settings. The concentration of the strain being tested could also be determined directly by comparison of the peak volumes of the test strain and the reference strain.

The measurements on a mixture of three cultured bacterial species are shown in Fig. 1. In the bivariate contour plot (Fig. 1a) each bacterial species forms a distinct cluster which carries several pieces of information. The radial coordinate is roughly proportional to the cellular DNA content. The radial extension of the cluster reflects increasing DNA content due to chromosome replication, incompletely separated cells, and possibly clumping. The angular displacement of a cluster from the vertical (H) axis is a function of the GC percentage. The three clusters are ordered as expected on the basis of the published values of GC percentages listed in Table 1. The cluster volumes are proportional to the bacterial concentrations. In Fig. 1b the distribution of the ratio of the two fluorescence signals, C/H, is shown. Information on DNA content is absent in this display, since all cells on a radial line of the contour plot have the same C/H ratio. The distribution is plotted as a function of the logarithm of C/H to show more clearly that the shapes and coefficients of variation of the three peaks (15 to 20 percent) are comparable. The three peaks are well separated, an indication that these three species with widely differing GC percentages are easy to resolve in a mixture.

The data for all six species are tabulated in Table 1, along with data on GC values found in *Bergey's Manual* (*6*).

Table 1. Bacterial species analyzed by dual-beam flow cytometry after staining with Hoechst 33258 and chromomycin A3.

Bacterial species	Description	GC (%)†	GC/AT‡	(C/H)§
Pseudomonas aeruginosa	Gram-negative rods	67	1.00	1.00
Klebsiella pneumoniae	Gram-negative rods	52–56	0.58	0.45
Escherichia coli	Gram-negative rods	50–51	0.50	0.31–0.41¶
*Escherichia coli**	Gram-negative rods	50–51	0.50	0.43–0.44 ‖
Escherichia coli	Gram-negative rods	50–51	0.50	0.40–0.42#
Streptococcus pyogenes	Gram-positive cocci	35–40	0.30	0.18
Streptococcus pneumoniae	Gram-positive cocci	39–42	0.33	0.13
Staphylococcus aureus	Gram-positive cocci	31–39	0.27	0.11

*All isolates were obtained from clinical specimens at the Microbiology Division, San Francisco General Hospital, San Francisco, except for these two *E. coli* samples obtained from the Meat Science Research Laboratory, Department of Agriculture. †Range found in *Bergey's Manual* (*6*). ‡As calculated from the midpoint of the range of values in *Bergey's Manual* (*6*) and normalized to unity for *P. aeruginosa*. §Fluorescence signal ratio normalized to unity for *P. aeruginosa*. Replicate measurements indicate a precision of approximately ± 10 percent (standard deviation/mean). ¶Range of values of four strains. ‖ Values for two strains. #Values for two infected urine specimens analyzed directly from patient urine sediment.

The value of C/H increases with increasing GC/AT percentages, as would be expected from the preference of chromomycin A3 for GC-rich DNA and Hoechst 33528 for AT-rich DNA. The fact that C/H increases faster than the GC/AT percentages is the result of the mechanism of stain binding (stretches of three base pairs are optimal) and energy transfer (*4*). Some details are not yet understood. We observe significant differences in C/H values among the strains of *E. coli* listed in Table 1. Although individual strains of *E. coli* differ slightly in GC percentage, it is possible that strain-to-strain differences in other biochemical characteristics may have some effect on C/H. The correlation of C/H and GC/AT values for *Streptococcus pyogenes, S. pneumoniae*, and *Staphylococcus aureus* is not clear-cut because of the wide range of literature values of GC percentages for these species.

Bacterial infection of urine specimens can be detected with a flow cytometer. The measured results on a urine specimen infected with *E. coli* (about 10^6 per milliliter) are shown in Fig. 1, c and d. A sample of cultured *P. aeruginosa* was added to the urine specimen to provide an internal calibration. The bacteria stain well and nonspecific staining of other particles or debris in the urine is minimal. The C/H of 0.42 (normalized to *P. aeruginosa*) falls within the range of values obtained from cultured strains of *E. coli* (Table 1). The coefficient of variation of the *E. coli* peaks in Fig. 1, b and d, are equal (14 to 15 percent). This shows comparable measurement resolution of *E. coli* from urine and cultured strains.

Our new flow cytometric method for bacterial characterization that is sensitive to DNA base composition adds a new dimension of specificity to flow cytometric methods for determining the cellular content of total nucleic acids, protein, and DNA. It has potential for the rapid counting and identification of bacteria in clinical, food, and environmental samples. The ability to measure mixtures of species may allow direct determination of the relative concentration and proliferative state of each species without the perturbations induced by methods dependent on culturing, which would be important in studies of microbial competition (*7*). The measurement of genome size and base composition of unknown strains may facilitate determination of phylogenetic relations. Specificity for bacterial identification may be further enhanced by the use of other optical probes such as fluorescent antibodies to surface antigens, fluorogenic substrates for proteases and other enzymes, fluorescent probes for total protein, fluorescein-conjugated lectins, and the scattering of linearly or circularly polarized light.

M. A. VAN DILLA
R. G. LANGLOIS
D. PINKEL
Biomedical Sciences Division, Lawrence Livermore National Laboratory, University of California, Livermore 94550

D. YAJKO
W. K. HADLEY
Department of Laboratory Medicine, University of California, San Francisco, and *Microbiology Division, San Francisco General Hospital, San Francisco 94110*

References and Notes

1. M. Melamed, P. Mullaney, M. Mendelsohn, *Flow Cytometry and Sorting* (Wiley, New York, 1979); P. K. Horan and L. L. Wheeless, Jr., *Science* **198**, 149 (1977).
2. K. Hutter and H. Eipel, *J. Gen. Microbiol.* **113**, 369 (1979); J. E. Bailey, J. Fazel-Madjlessi, D. N. McQuitty, L. Y. Lee, J. C. Allred, J. A. Oro, *Science* **198**, 1175 (1977); A. Paau, J. Oro, J.

Cowles, *Plant Physiol.* **63**, 402 (1979); R. Howard, F. Battye, G. Mitchell, *J. Histochem. Cytochem.* **27**, 803 (1979); H. Steen, E. Brye, K. Skarstad, B. Bloom, T. Godal, S. Mustafa, *Cytometry* **2**, 249 (1982).
3. R. Douglas and C. Ballou, *J. Biol. Chem.* **255**, 5979 (1980).
4. R. Langlois, A. Carrano, J. Gray, M. Van Dilla, *Chromosoma* **77**, 229 (1980).
5. P. Dean, in *Flow Cytometry*, O. Laerum, T. Lindmo, E. Thorud, Eds. (Universitetsforlaget, Oslo, 1980), vol. 4, pp. 41–44; P. Dean and D. Pinkel, *J. Histochem. Cytochem.* **26**, 622 (1978).
6. *Bergey's Manual of Determinative Bacteriology*, R. Buchanan and N. Gibbons, Eds. (Williams and Wilkins, Baltimore, ed. 8, 1974).
7. A. G. Fredrickson and G. Stephanopoulos, *Science* **213**, 972 (1981).
8. This work was performed under the auspices of the Department of Energy by the Lawrence Livermore National Laboratory under contract W-7405-ENG-48.

28 June 1982; revised 30 November 1982

Interrelated Striated Elements in Vestibular Hair Cells of the Rat

Abstract. *Unusual fixation procedures revealed a series of interrelated striated organelles in type I and type II vestibular hair cells of the rat; these organelles seemed to be less well developed in cochlear hair cells. The findings suggest that contractile elements may play a role in sensory transduction in the inner ear, particularly in the vestibular system.*

Actin is present in the hair cells of vestibular (*1*, *2*) and auditory (*3*, *4*) receptors. By S-1 myosin decoration methods (*5*), actin has been found in the stereocilia and their rootlets, the cuticular plate, and the electron-opaque material that forms the junctional complexes of the reticular lamina. Because myosin also has been found in apical parts of hair cells of the organ of Corti (*6*), it might be expected that actin and myosin are organized into contractile elements that take part in signal processing in the inner ear. Generally, however, S-1 myosin decoration has failed to demonstrate highly organized actin filaments in the cuticular plate (*1–4*). Only Slepecky and her colleagues (*7*) have illustrated an infracuticular, striated element containing actin (*4*). Lowenstein and Osborne (*8*) earlier described ribbonlike striated elements in vestibular hair cells of ammocoetes larvae of the lamprey extending from the cuticular plate to the cell membrane basally and ending close to synaptic sites. Their results, obtained by conventional transmission electron microscopy, prompted them to hypothesize that such striated material might be involved in transduction. Other investigators have also reported finding isolated laminated, or striated, elements in the basal part of the cuticular plate, or below it, in hair cells of both normal (*9–14*) and pathological (*9*, *15*) inner ears in many species. Striated material was also abundant in hair cells of old monkeys (*12*) and elderly humans (*12*, *16*), and in drug-treated animals (*13*, *17*). The apparently increased incidence of such bodies under pathological conditions and as a consequence of aging seems to have overshadowed findings in normal material, and laminated bodies have generally come to be regarded as pathological entities. Nevertheless, several investigators have emphasized that striated elements are normal constituents of vestibular (*8*, *10–12*) and cochlear (*7*, *14*) hair cells.

We now describe our ultrastructural finding of a series of interrelated striated elements in apical parts of vestibular hair cells of the rat. Included in the series are the cuticular plate and its basal attachments to the hair cell margins, the connections of the strut array of the kinociliary basal body (*18*) to the cuticular plate, and striated organelles associated with the plasma membrane and extending below the apical junctional complexes. The latter organelles are more extensive in type I than in type II hair cells. In contrast, rat cochlear hair cells seem to lack similar striated organelles associated with the plasma membrane and to have less robust striations in the cuticular plate. Our findings indicate a broader distribution of striated elements in vestibular hair cells than was found previously. They support the concept that contractile elements may play a role in transduction in the inner ear (*7*, *8*, *19*), particularly in the vestibular system.

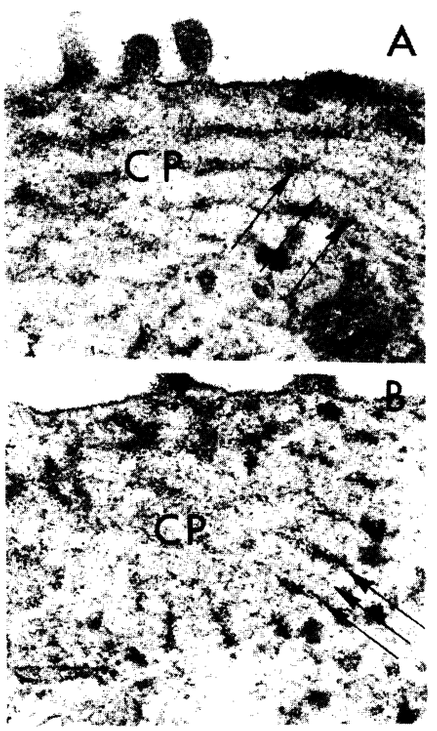

Fig. 1. (A) Striations in the substance of the cuticular plate (*CP*) of a type I utricular hair cell. (B) Striations along the lower face of the circular plate of a type II utricular hair cell. The three arrows indicate opposite electron-opaque stripes and an intermediate line. Magnification: ×43,000.

Our results were obtained in specific-pathogen-free, young adult, Sprague-Dawley rats (Charles River) during an effort to determine an optimal method for preserving inner ear tissue collected under space-flight conditions. Osmium tetroxide could not be used, because of its toxicity; tissues, once collected, might have to be stored for as long as 5 days before further processing could take place. The following method resulted in unexpected preservation of the striated organelles in hair cells. Temporal bones were rapidly removed from decapitated rats, and the oval and round windows of the cochleas were opened immediately upon immersion in 2.5 percent glutaraldehyde in 0.1*M* sodium phosphate buffer (*p*H 7.4). After fixation for 2 hours at room temperature, the tissues were stored in fresh fixative in vials at 4°C for 5 days. The tissues were then washed in buffer, fixed in 1.0 percent osmium tetroxide in 0.1*M* sodium phosphate buffer (*p*H 7.4) for 1 hour, then washed again, microdissected, and prepared by standard methods for transmission electron microscopy. Subsequent experiments demonstrated that the striated organelles were well preserved when prolonged storage was omitted. The organelles were not seen, however, after fixation in Karnovsky's (*20*) 4 percent paraformaldehyde–5 percent glutaraldehyde solution.

The striated organelles of hair cells have a repeating pattern of alternating electron-opaque stripes and broader, more electron-lucent bands. The bands are intersected by narrow, electron-opaque, intermediate lines (Figs. 1 and 2). This pattern is organizationally similar to that of striated rootlets of the kinociliary basal body in the hair cells themselves, and particularly to that described for contractile rhizoplasts in the flagellate *Platymonas subcordiformis* (*21*). It is also comparable to the pattern commonly reported for isolated laminat-